Am J Transl Res 2023;15(6):3928-3941
www.ajtr.org /ISSN:1943-8141/AJTR0149761

Original Article

MALAT1 knockdown alleviates myocardial injury in mice with severe acute pancreatitis via the miR-374a/Sp1/Wnt/β-catenin pathway

Yan Sun[1], Renlian Gu[2], Zhong Shen[1], Yanshuo Ye[3]

[1]Department of General Surgery, Jinshan Branch of Shanghai Sixth People's Hospital, Shanghai Jiaotong University, Shanghai 201599, P. R. China; [2]Department of Emergency, Jinshan Branch of Shanghai Sixth People's Hospital, Shanghai Jiaotong University, Shanghai 201599, P. R. China; [3]Department of General Surgery, The Third Affiliated Hospital of Jilin University, Changchun 130021, Jilin, P. R. China

Received February 20, 2023; Accepted May 18, 2023; Epub June 15, 2023; Published June 30, 2023

Abstract: Background: Severe acute pancreatitis (SAP) contributes to high mortality (as high as 30%) and multiple organ injuries. In this study, we established a mouse model with SAP to detect biomolecules implicated in myocardial injury and to expound the signal transduction pathway involved. Methods: A SAP mouse model was established to assess inflammation- and myocardial injury-related markers. Also, pancreatic and myocardial injuries and cardiomyocyte apoptosis were evaluated. Microarray analysis was implemented to filter differentially expressed long non-coding RNAs (lncRNAs) in myocardial tissues of normal and SAP mice. Then, miRNA-based microarray analysis and bioinformatics prediction were performed to probe the downstream molecules of MALAT1, followed by rescue experiments. Results: SAP mice showed pancreatic and myocardial injuries and increased apoptosis of cardiomyocytes. MALAT1 was expressed highly in SAP mice, and inhibition of MALAT1 reduced myocardial injury and cardiomyocyte apoptosis in SAP mice. MALAT1 was found to localize to the cytoplasm of cardiomyocytes and bind to miR-374a. Inhibition of miR-374a inhibited the alleviating effects of MALAT1 knockdown on the myocardial injury. miR-374a targeted Sp1, and Sp1 silencing reversed the promoting effects of miR-374a inhibitor on myocardial injury. Sp1 regulated myocardial injury in SAP via the Wnt/β-catenin pathway. Conclusion: MALAT1 promotes myocardial injury complicated by SAP via the miR-374a/Sp1/Wnt/β-catenin pathway.

Keywords: Long non-coding RNA MALAT1, microRNA-374a, Sp1, Wnt/β-catenin pathway, severe acute pancreatitis, myocardial injury

Introduction

Acute pancreatitis (AP), a mild self-limiting disorder, poses a great burden for global morbidity and mortality, and the annual incidence seems to be on a rise [1]. The most common causes for AP are gallstones (accounting for 40-65%) and alcohol consumption (25-40%), and the remaining 10 to 30% of cases are attributed to various causes including autoimmune and genetic risk factors [2]. Severe AP (SAP) runs a biphasic course, contributing to a systemic inflammatory response, which may result in early multisystem organ (respiratory, cardiovascular, renal, and hepatic) failure [3]. Cardiovascular dysfunction might be observed throughout the clinical course of SAP [4]. Therefore, a better understanding of the mechanisms underlying the occurrence of myocardial injury in SAP represents a necessity to offer more accurate diagnoses and effective treatment options to combat the disease.

Long non-coding RNAs (lncRNAs) are around 200 nucleotides (nts) in length and exert important roles in a multitude of biological processes [5]. More recently, their functions have been indicated in AP. For instance, lncRNA Fendrr was upregulated in the AP cell model and bound to Annexin A2 protein directly to facilitate the apoptosis of AR42J cells [6]. In addition, lncRNA intersectin 1-2 was increased in SAP patients compared with moderate-AP patients, mild AP patients, and healthy controls, which

makes it a possible biomarker for discrimination of SAP [7]. To clarify the finer mechanism of the lncRNA involvement in myocardial injury caused by SAP, we conducted a microarray analysis, which revealed that metastasis-associated lung adenocarcinoma transcript 1 (MALAT1) was the most significantly upregulated lncRNA in myocardial tissues of SAP mice. MALAT1 is among the most abundantly expressed lncRNA in numerous cancers [8]. Moreover, silencing of MALAT1 reduced the apoptosis of cardiomyocytes and brain microvascular endothelial cells, thus being involved in left ventricular function [9] and ischemic stroke [10]. However, its relevance to SAP-induced myocardial injury has been rarely investigated. microRNAs (miRNAs) are a group of non-coding RNAs (~22 nts) that post-transcriptionally regulate protein-coding genes via mRNA cleavage, direct translational repression as well as mRNA destabilization, and lncRNAs can serve as miRNA sponges, controlling their regulatory effect on mRNAs [11]. This led to a hypothesis that the effect of MALAT1 on SAP-induced myocardial injury may be associated with a certain miRNA and its target mRNA. Here, we set to elucidate the dysregulation and underlying effects of MALAT1 in an SAP mouse model, aiming to provide putative therapeutic targets for SAP.

Materials and methods

Animal models

Animal experiments were conducted following the animal care guidelines of the Chinese National Institutes of Health and approved by the Animal Care and Use Committee of Shanghai Sixth People's Hospital (Approval No. SYXK2021-0028). Forty C57BL/6N mice were purchased from Beijing Vital River Laboratory Animal Technology Co., Ltd. (Beijing, China). All mice were kept in the laboratory for at least 5 days to acclimatize.

The mice were anesthetized by intraperitoneal injection of 1% pentobarbital sodium (50 mg/kg) under aseptic conditions. A total of 35 mice were modeled with SAP. After immobilization of the mice, an incision was made in the middle of the upper abdomen to expose the hepatic hilum. The biliopancreatic duct near the hepatic hilum was clamped. A needle punctured the duodenal wall into the intestinal cavity and was inserted into the biliopancreatic duct retrograde through the opening of the duodenal papilla to prevent reflux. Thereafter, 5% sodium taurocholate (Sigma-Aldrich Chemical Company, St. Louis, MO, USA) was injected into the pancreatic duct. After the injection, the needle was kept in place for 5 min until there was visible edema and bleeding in the pancreatic tissues. Then, the needle was removed, followed by suture of the incision and closing of the abdomen. After awakening from anesthesia, the mice drank and ate freely for subsequent experiments. Sham-operated mice (n = 5) were subjected to the same procedure, and the injection solution was changed to saline [12]. The successful establishment of the SAP mouse model was verified by measuring serum amylase content through standard photometric reactions using a spectrophotometer.

Plasmid delivery

Small interfering (si) RNA-MALAT1 and MALAT1-negative control (NC), miR-374a control and miR-374a inhibitor, si-Sp1 and Sp1-NC fragments were synthesized by GenePharma (Shanghai, China), and low expression plasmids were generated by recombinant adenovirus AD-CMV-Cre (Vector BioLabs, Philadelphia, PA, USA). At the 10^{th} d before SAP induction, si-MALAT1 (1×10^9 PFU), MALAT1-NC, si-MALAT1 + miR-374a control, si-MALAT1 + miR-374a inhibitor, miR-374a inhibitor + Sp1-NC, or miR-374a inhibitor + si-Sp1 was intravenously injected into mice (n = 5) for five times at an interval of two days, and the control mice received empty adenoviral vectors for subsequent experiments. The RNAi sequences used are listed in **Table 1**.

Enzyme-linked immunosorbent assays (ELISA)

The serum of mice was collected by centrifugation at 3000 r/min at 4°C for 10 min. The kits for tumor necrosis factor-α (TNF-α, CSB-E04741m, Cusabio Biotech, Newark, DE, USA), interleukin-6 (IL-6, CSB-E04639m, Cusabio Biotech), cardiac troponin-T (cTnT, E-EL-M18-01c, Elabscience Biotechnology Co., Ltd., Wuhan, Hubei, China), creatine kinase isoenzyme (CK-MB, ab285231, Abcam Inc., Cambridge, UK), and lactate dehydrogenase (LDH, E-EL-M0419c, Elabscience) were purchased, and all operations were carried out according to the manufacturer's protocols.

Table 1. RNAi sequence used for regulated gene

siRNA	Guide sequences (5'-3')	Passenger sequences (5'-3')
MALAT1-NC	AAAAGACUGGGAGAAAGAGCC	CUCUUUCUCCCAGUCUUUUUU
si-MALAT1	ACUUAUCUGCGAUUUCCUCGG	GAGGAAAUCGCAGAUAAGUUU
SP1-NC	UUUCAAACGAGAAGUAGUCCC	GACUACUUCUCGUUUGAAAGU
si-Sp1	AACAUCUUUUUCAAUCUUCAC	GAAGAUUGAAAAAGAUGUUGG
miR-374a Control	AGUGUACCAGCUUGGCCACAAC	
miR-374a inhibitor	CACUUAUCAGGUUGUAUUAUAA	

Note: siRNA, small interfering RNA; MALAT1, metastasis-associated lung adenocarcinoma transcript 1; miR, microRNA.

Pancreatic water content

Mice were euthanized by intraperitoneal injection of 1% sodium pentobarbital (150 mg/kg, Biochem, Wuhan, Hubei, China) after 24 h. The pancreatic tissues were removed and washed with saline. Freshly harvested tissues (wet weight) were weighed, quantified, and compared with the weight of the same samples after drying at 160°C for 48 h (dry weight). The pancreatic water content was expressed as a percentage: (wet weight - dry weight)/wet weight × 100%.

Hematoxylin-eosin (HE) staining

HE staining was performed to assess pancreatic and myocardial tissue injury in mice. The pancreatic and myocardial tissues were fixed in 10% formalin at 4°C overnight, then dehydrated, paraffin-embedded, and cut into 4-μm sections. The sections were then hydrated, stained with hematoxylin (Beijing Solabio Life Sciences Co., Ltd., Beijing, China) for 12 min, and differentiated with 1% hydrochloric alcohol for 10 s. After being rinsed with tap water for 40 min, the sections were stained in eosin (Solabio) for 4 min, dehydrated, then cleared with xylene I and xylene II, respectively, sealed with resin and observed under the microscope. Tissue structural changes were observed with an optical microscope (Zeiss, Oberkochen, Germany). The pathological injury score was evaluated from edema (0-4 score), inflammation (0-4 score), and necrosis (0-4 score) as described by a previous report [13], and the final score was the sum of the three scores.

TUNEL assay

Myocardial tissues were fixed overnight at 4°C in 10% formalin, sectioned, and stained with a commercial TUNEL kit (MK1025, Wuhan Boster Biological Technology Co., Ltd., Wuhan, Hubei, China). The sections were incubated with a blocking reagent contained in the kit for 1 h and then with TdT, digitonin-11-dUTP (DIG-dUTP), biotinylated anti-digoxin antibody, and SABC. The sections were developed using DAB and sealed with neutral resin, and the resulting sections were examined under a microscope (Zeiss). TUNEL activity (active cells/total cells × 100%) was calculated.

Microarray analysis

Mouse myocardial tissues were obtained, and total RNA was extracted using TRIzol reagent (Thermo Fisher Scientific Inc., Waltham, MA, USA). The RNA was synthesized into complementary deoxyribonucleic acid (cDNA) using HiScript 1st Strand cDNA Synthesis Kit (Nanjing Vazyme Biotech Co., Ltd., Nanjing, China). Fluorescently labeled lncRNAs were hybridized with Mouse V4.0 LncRNA Array (Arraystar Inc., Rockville, MD, USA). Fluorescently labeled miRNAs were hybridized using SurePrint mouse miRNA microarrays (Agilent Technologies, Santa Clara, CA, USA). The data were scanned with a GeneChip™ Scanner 3000 7G system (Thermo Fisher Scientific) and analyzed using Expression Console Software. Robust multichip analysis was performed for background correct and raw data normalization. $P < 0.01$ and |Fold change| > 2 were used to define differentially expressed lncRNAs/miRNAs and to plot the heatmaps.

Reverse transcription-quantitative polymerase chain reaction (RT-qPCR)

Total RNA was extracted using TRIzol reagent (Thermo Fisher). RNA concentration was measured using a Nanodrop spectrophotometer

Table 2. Primer sequences

Gene name	Primer sequences
MALAT1	F-5'-TGCAGTGTGCCAATGTTTCG-3'
	R-5'-GGCCAGCTGCAAACATTCAA-3'
Sp1	F-5'-CTCCAGACCATTAACCTCAGTGC-3'
	R-5'-CACCACCAGATCCATGAAGACC-3'
hsa-β-actin	F-5'-CACCATTGGCAATGAGCGGTTC-3'
	R-5'-AGGTCTTTGCGGATGTCCACGT-3'
GAPDH	F-5'-CATCACTGCCACCCAGAAGACTG-3'
	R-5'-ATGCCAGTGAGCTTCCCGTTCAG-3'
U6	F-5'-CTCGCTTCGGCAGCACAT-3'
	R-5'-TTTGCGTGTCATCCTTGCG-3'
miR-374a	F-5'-TATAATACAACCTGATAAGTG-3'
	R-5'-GAACATGTCTGCGTATCTC-3'

Note: MALAT1, metastasis-associated lung adenocarcinoma transcript 1; hsa, homo sapiens; mmu, mus musculus; miR, microRNA; F, forward; R, reverse.

(Thermo Fisher). The cDNA was reversely transcribed from total RNA using a HiScript 1st Strand cDNA Synthesis Kit (Vazyme), and cDNA was generated from miRNA using the stem-loop RT-qPCR method. In the ABI StepOnePlus real-time PCR system (Applied Biosystems, Inc., Foster City, CA, USA), β-actin and U6 were used as endogenous controls in the mRNA and miRNA expression profiles, respectively. The $2^{-\Delta\Delta CT}$ method was utilized to calculate the relative quantification. The primers for this study are displayed in **Table 2**.

Western blot

Myocardial tissues were lysed in radioimmunoprecipitation assay (RIPA) lysis buffer (Thermo Scientific) on ice for 30 min. The lysates were centrifuged at 12,000 rpm for 0.5 h at 4°C, and the protein concentration was determined by using a bicinchoninic acid protein assay kit (Beyotime, Shanghai, China). Equal amounts of protein (20 μg) were subjected to 12% sodium dodecyl sulfate-polyacrylamide gel electrophoresis. The protein was then electrically transferred to a polyvinylidene fluoride membrane (Millipore, Billerica, MA, USA), blocked for 1 h with 5% bovine serum albumin at room temperature, and incubated after the addition of Bcl-2 (1:500, 26593-1-AP, ProteinTech Group, Chicago, IL, USA), Bax (1:400, 50599-2-Ig, ProteinTech), β-catenin (1:2500, #AF0066, Beyotime), Wnt1 (1:500, #A00354, Boster), and GAPDH (1:2000, ab9485, Abcam) at 4°C overnight. Thereafter, filters were treated with the corresponding horseradish peroxidase-labeled secondary antibody (1:2000, ab6721, Abcam) at room temperature for 60 min and developed with enhanced chemiluminescence (Beyotime) and quantified using Quantity One (Bio-Rad Laboratories, Hercules, CA, USA).

Subcellular fractionation

Human cardiac myocytes (HCM, Procell, Wuhan, Hubei, China) were cultured in DMEM containing 10% FBS (Thermo Fisher Scientific) and resuspended with Hypotonic buffer A containing protease inhibitor and RNase inhibitor (Thermo Fisher Scientific), incubated on ice for 10 min and then centrifuged at 1000 × g for 10 min at 4°C. The supernatant was further centrifuged at 15,000 × g for 15 min, and the cytoplasmic fraction was obtained. The precipitate was rinsed with a hypotonic buffer, resuspended again, then centrifuged at 6000 × g for 10 min at 4°C. The obtained precipitate was resuspended with RIPA buffer containing protease inhibitor and RNase inhibitor, incubated at 4°C for 30 min, centrifuged at 15000 × g for 20 min, and the supernatant was the nuclear fraction. PCR was then conducted to determine the expression of U6, GAPDH, and MALAT1 in the cell cytoplasm and nuclei.

Dual-luciferase reporter gene assay

TargetScan (http://www.targetscan.org/), StarBase (http://starbase.sysu.edu.cn/), mirDIP (http://ophid.utoronto.ca/mirDIP/index.jsp#r), miRTarBase (https://mirtarbase.cuhk.edu.cn/~miRTarBase/miRTarBase_2022/php/index.php), miRDB (http://www.mirdb.org/) were used to predict the target genes of miR-374a. StarBase predicted the binding sites of MALAT1 to miR-374a, followed by luciferase reporter gene assays to confirm whether miR-374a is a target of MALAT1 and Sp1 is a target of miR-374a. The sequences of the binding sites to miR-374a binding sites in MALAT1/Sp1 RNA were amplified by PCR and mixed with the pmirGLO vector (Promega Corporation, Madison, WI, USA). The wild-type (WT) reporter gene was constructed and named MALAT1/Sp1-WT, and the pGL3 MALAT1/Sp1 mutant (MT) reporter gene containing the seed sequence point mutation was generated using

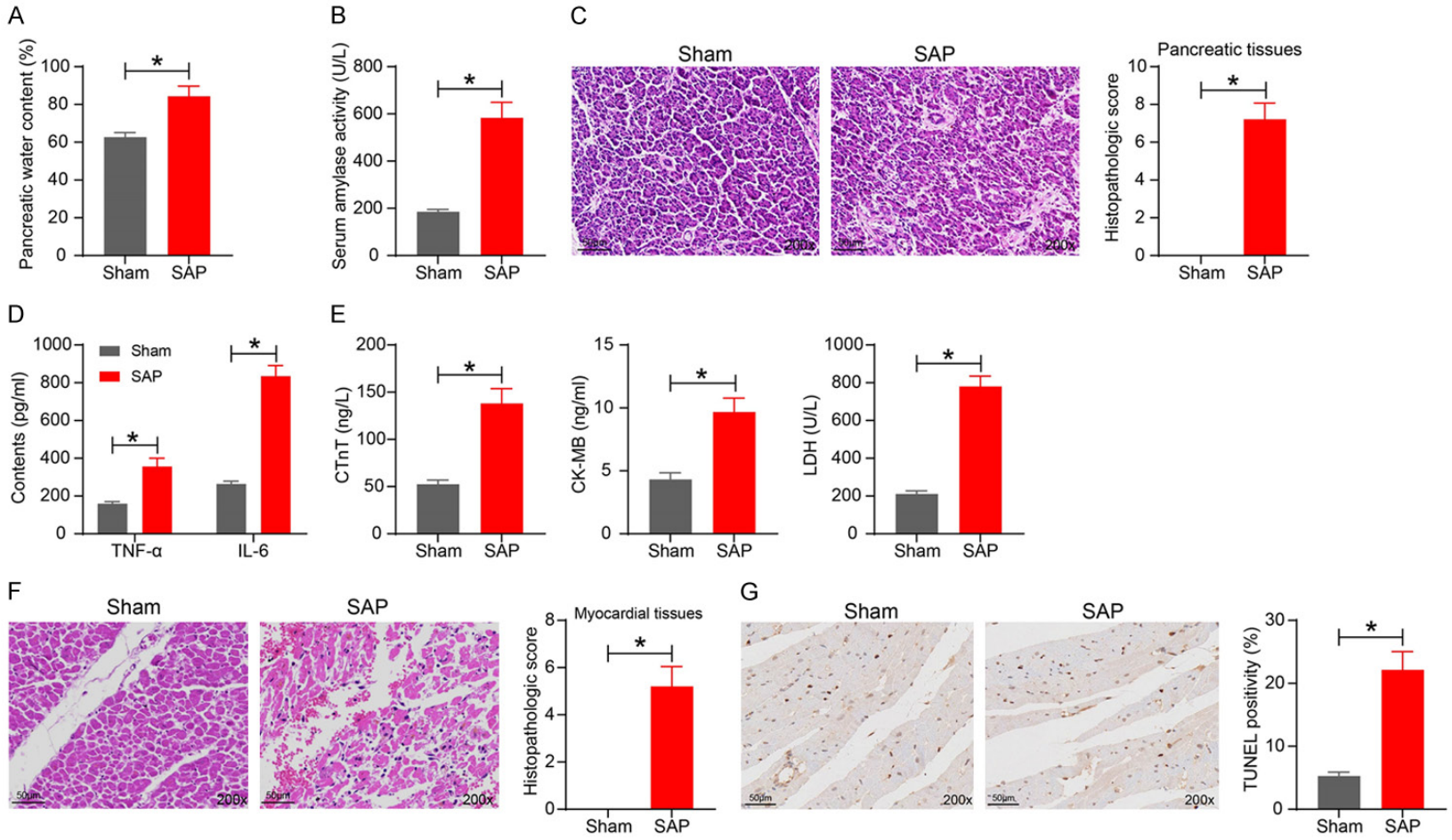

Figure 1. SAP mice showed myocardial injury. (A) Pancreatic water content in SAP mice; (B) Determination of serum amylase activity by colorimetric assay; (C) HE staining for determine pancreas damage; (D) ELISA for the detection of inflammatory factors in the blood of mice; (E) ELISA for the detection of myocardial injury markers in mouse blood; (F) Observation of damage in myocardial tissues of SAP mice by HE staining; (G) Observation of cardiomyocyte apoptosis in mouse myocardial tissues by TUNEL. n = 5. Measurement data were expressed as mean ± standard deviation; an unpaired *t-test* was performed for comparisons between two groups (A-C, E and G), and the two-way ANOVA was performed for multiple-group comparison (D); the experiment was repeated three times. $^{*}P < 0.05$ *vs.* the sham group. SAP, severe acute pancreatitis; ELISA, enzyme-linked immunosorbent assays; HE, hematoxylin-eosin; TUNEL, terminal deoxynucleotidyl transferase (TDT)-mediated 2'-deoxyuridine 5'-triphosphate (dUTP) nick end labeling; ANOVA, analysis of variance.

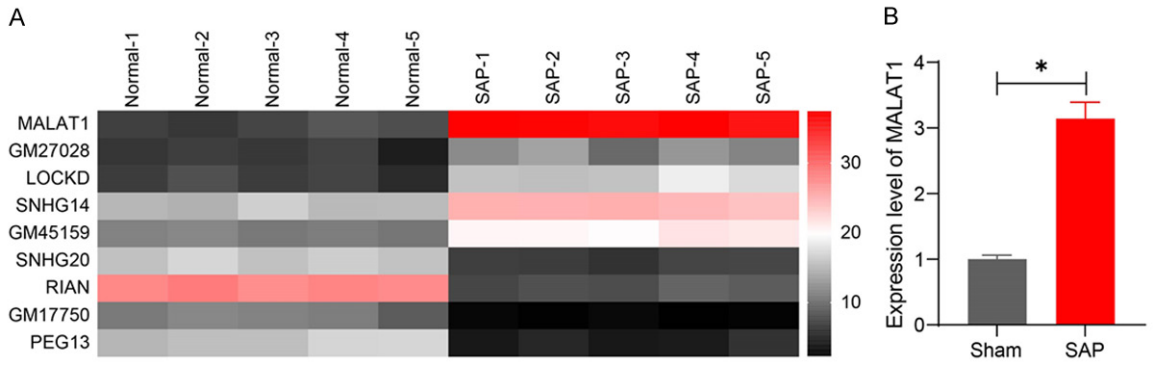

Figure 2. MALAT1 was overexpressed in injured myocardial tissues caused by SAP. (A) Microarray analysis of differentially expressed lncRNAs in myocardial tissues from SAP and sham-operated mouse tissues; (B) MALAT1 expression in SAP and sham-operated mouse myocardial tissues detected by RT-qPCR (n = 5). Measurement data were expressed as mean ± standard deviation; an unpaired *t-test* was performed for comparisons between two groups (B). $^{*}P < 0.05$ *vs.* the sham group. SAP, severe acute pancreatitis; MALAT1, metastasis-associated lung adenocarcinoma transcript 1; RT-qPCR, reverse transcription-quantitative polymerase chain reaction.

a site-directed mutagenesis kit (Stratagene, La Jolla, CA, USA) and named MALAT1/Sp1-MT. HCM were co-transfected with miR-374a inhibitor and control and reporter genes and incubated for 48 h, and the luciferase activity of each group of cells was evaluated by the dual-luciferase reporter gene assay system (Promega).

Statistical analysis

SPSS 22.0 software (IBM Corp., Armonk, NY, USA) was applied for statistical analysis. Measurement data were expressed as mean ± standard deviation. Comparisons between two groups were analyzed using the unpaired *t-test*, while comparisons among multiple groups were performed with one-way or two-way analysis of variance (ANOVA), followed by Tukey's post hoc test. $P < 0.05$ was indicative of statistical significance.

Results

SAP induced myocardial injury in mice

Firstly, we developed an SAP mouse model by sodium taurocholate injection, and then we verified the successful establishment of SAP mice through a series of experiments. The comparison of pancreatic water content between SAP mice and normal mice revealed that the pancreatic water content of SAP mice was significantly increased (**Figure 1A**). Fasting blood of mice was collected, and serum amylase activity was significantly increased in SAP mice (**Figure 1B**). The damage of the pancreatic tissues was assessed by the structural changes, which were characterized by vacuolization of follicular cells, neutrophilic infiltration around blood vessels, the presence of necrotic cells, and obvious pancreatic edema in SAP mice induced by sodium taurocholate. Significantly higher pathology scores were also observed in SAP mice (**Figure 1C**).

The contents of TNF-α and IL-6 were increased in SAP mice compared with sham-operated mice (**Figure 1D**). The levels of cTnT, CK-MB, and LDH in the blood of the SAP mice were also increased, and the level of LDH in the blood of SAP mice was much higher than that of the sham-operated mice (**Figure 1E**). Meanwhile, HE staining demonstrated that after SAP induction, myofibrils were broken and separated, endothelial cells and capillaries were damaged, and cells showed edema and inflammatory cell infiltration (**Figure 1F**). The results of TUNEL assays showed that the apoptosis of cardiomyocytes was significantly increased in SAP mice, and the activity of cardiomyocytes in tissues was decreased (**Figure 1G**).

MALAT1 was upregulated in injured myocardial tissues caused by SAP

After observing pancreatitis and myocardial injuries in SAP mice, we detected the differentially expressed lncRNAs in the injured and con-

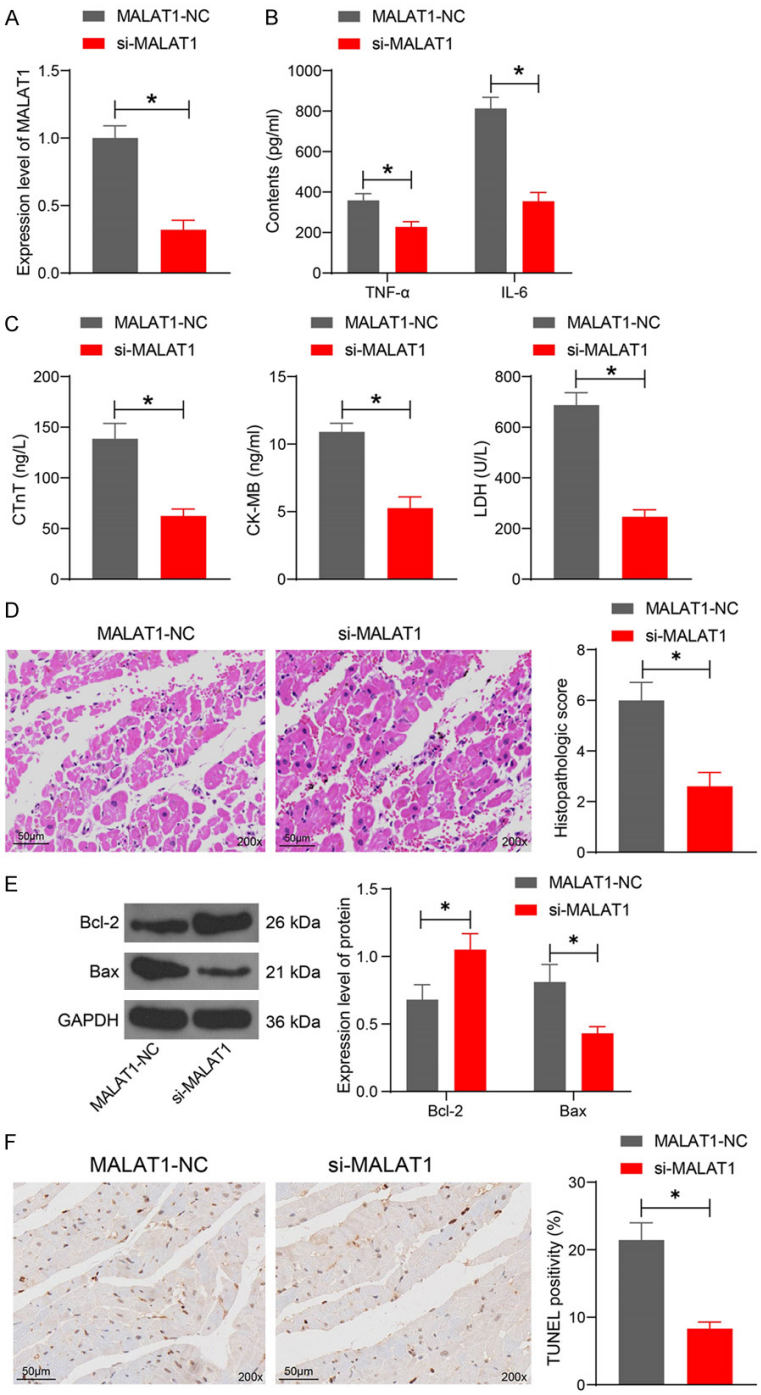

Figure 3. Downregulation of MALAT1 protected the SAP mice against myocardial injury. SAP mice were delivered with si-MALAT1 or MALAT1-NC. (A) RT-qPCR to assess the efficiency of si-MALAT1; (B) ELISA for the detection of inflammatory factors in the blood of mice; (C) ELISA for the detection of myocardial injury markers in mouse myocardial tissue; (D) Observation of damage in myocardial tissue of SAP mice by HE staining; (E) Western blot detection of apoptotic proteins Bcl-2 and Bax in myocardial tissues of SAP mice; (F) Observation of cardiomyocyte apoptosis in myocardial tissues by TUNEL staining. n = 5. Measurement data were expressed as mean ± standard deviation; an unpaired *t-test* was performed for comparisons between two groups (A, C, D and F), and the two-way ANOVA was performed for multiple-group comparison (B and E); the experiment was repeated three times. *$P < 0.05$ *vs.* the MALAT1-NC group. SAP, severe acute pancreatitis; MALAT1, metastasis-associated lung adenocarcinoma transcript 1; RT-qPCR, reverse transcription-quantitative polymerase chain reaction; ELISA, enzyme-linked immunosorbent assays; HE, hematoxylin-eosin; TUNEL, terminal deoxynucleotidyl transferase (TDT)-mediated 2'-deoxyuridine 5'-triphosphate (dUTP) nick end labeling; ANOVA, analysis of variance.

trol healthy myocardial tissues by microarray analysis. By plotting the heatmap, we found that MALAT1 was significantly overexpressed in the injured myocardial tissues of SAP mice (**Figure 2A**). A high expression of MALAT1 was observed in the myocardial tissues of SAP mice, as revealed by RT-qPCR (**Figure 2B**).

MALAT1 knockdown alleviated myocardial injury in SAP mice

A lentiviral vector was used to deliver the si-MALAT1 fragment into mice, which were then induced with SAP, and myocardial tissues were collected after the euthanasia. MALAT1 expression in the myocardial tissues of mice administrated with si-MALAT1 was first quantified by PCR, which was significantly decreased compared with mice delivered with MALAT1-NC (**Figure 3A**). Detection of pro-inflammatory factors in myocardial tissue with or without MALAT1 knockdown displayed that downregulation of MALAT1 decreased the levels of pro-inflammatory factors in mouse myocardial tissues (**Figure 3B**). The detection of myocardial injury markers in tissues revealed that CTnT,

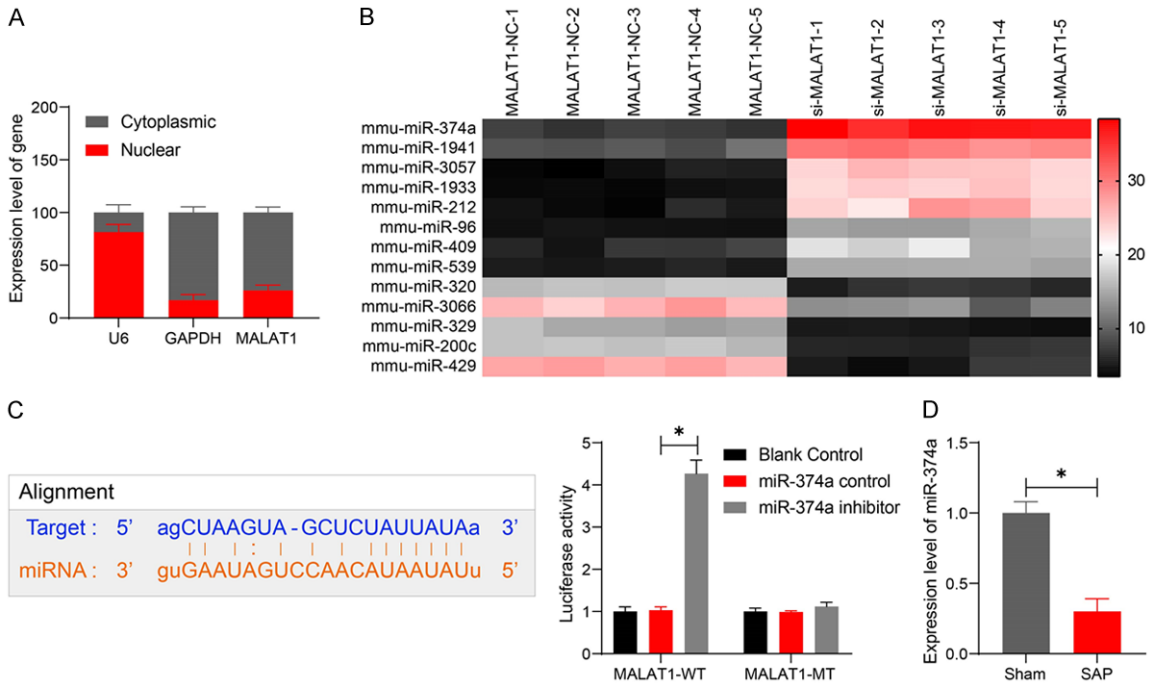

Figure 4. miR-374a is a downstream biomolecule of MALAT1. (A) Localization of MALAT1 in cardiomyocytes by subcellular fractionation assay; (B) Differentially expressed miRNAs after MALAT1 knockdown in mice screened out by microarray analysis (n = 5); (C) The binding relationship between MALAT1 and miR-374a verified by dual-luciferase assay; (D) Expression of miR-374a detected by RT-qPCR in SAP mice (n = 5). Measurement data were expressed as mean ± standard deviation; an unpaired *t-test* was performed for comparisons between two groups (D), and the two-way ANOVA was performed for multiple-group comparison (C); the experiment was repeated three times. $^{*}P < 0.05$ *vs.* the miR-374a control, or sham group. SAP, severe acute pancreatitis; MALAT1, metastasis-associated lung adenocarcinoma transcript 1; miR, microRNA; RT-qPCR, reverse transcription-quantitative polymerase chain reaction; ANOVA, analysis of variance.

CK-MB, and LDH showed a downward trend after MALAT1 downregulation (**Figure 3C**). The SAP mice with MALAT1 knockdown had different degrees of reduction in myocardial tissue injury and inflammatory cell infiltration (**Figure 3D**). The expression of apoptotic proteins Bcl-2 and Bax was assessed in tissues. Elevated Bcl-2 expression and decreased Bax expression in myocardial tissues after MALAT1 downregulation indicated that cardiomyocyte apoptosis was reduced by MALAT1 downregulation (**Figure 3E**). Finally, it was found that the TUNEL-positive rate was decreased in the myocardial tissues of mice with MALAT1 downregulation (**Figure 3F**).

MALAT1 regulated miR-374a expression through direct binding

Next, we explored the molecular mechanism of MALAT1 in myocardial injury and quantified the MALAT1 expression in the cytoplasm and nucleus of HCM by subcellular fractionation assay. MALAT1 was predominantly found in the cytoplasm of HCM (**Figure 4A**). We performed miRNA-based microarray analysis in myocardial tissues from MALAT1 overexpressing and control mice to investigate the downstream miRNAs affected by MALAT1. miR-374a expression exhibited the greatest change in mouse myocardial tissues after MALAT1 knockdown (**Figure 4B**). The targeting relationship between MALAT1 and miR-374a was verified by dual-luciferase experiments, and the luciferase activity of the MALAT1-WT plasmid was significantly increased after the downregulation of miR-374a (**Figure 4C**). Subsequent RT-qPCR revealed that the expression of miR-374a was significantly decreased in SAP-induced mice relative to sham-operated mice (**Figure 4D**).

miR-374a targeted and bound to Sp1

We then analyzed the downstream genes of miR-374a via the bioinformatic websites for intersection (**Figure 5A**). We tested the mRNA

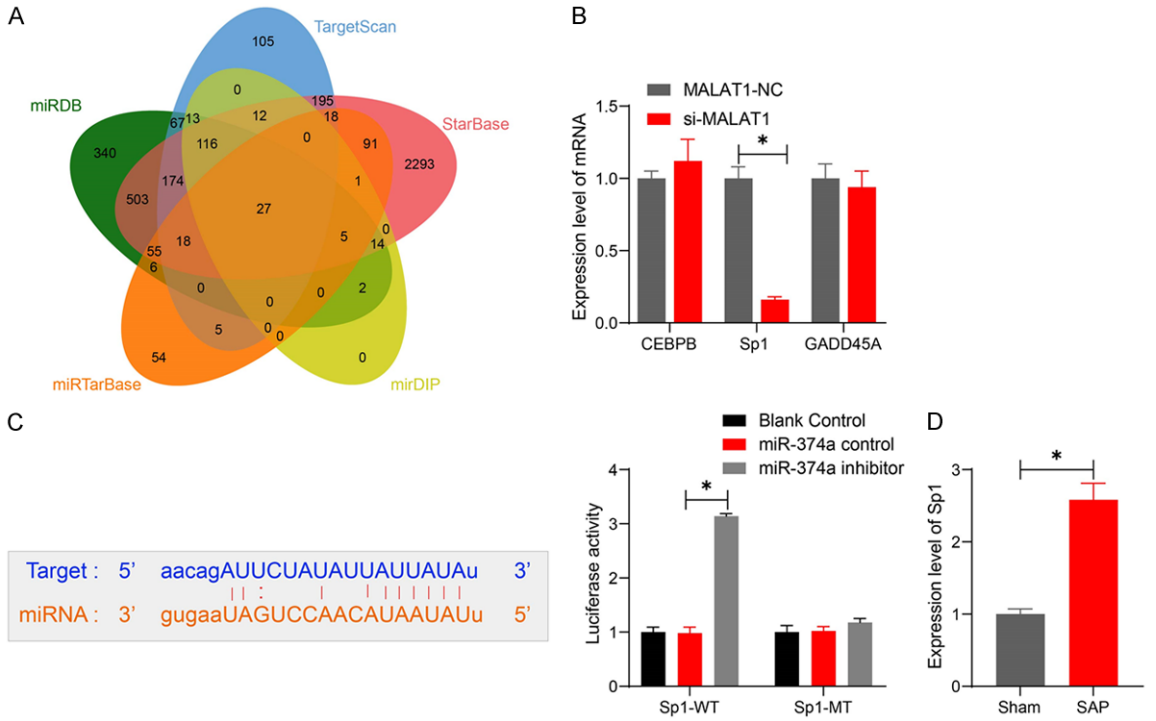

Figure 5. Sp1 was verified to be a possible target of miR-374a. (A) Screening for target genes of miR-374a by bioinformatics analysis; (B) Quantification of gene expression by RT-qPCR in SAP mice with low MALAT1 expression; (C) The binding relationship between Sp1 and miR-374a verified by dual-luciferase assay; (D) Expression of Sp1 detected by RT-qPCR in SAP mice (n = 5). Measurement data were expressed as mean ± standard deviation; an unpaired *t-test* was performed for comparisons between two groups (D), and the two-way ANOVA was performed for multiple-group comparison (B and C); the experiment was repeated three times. $^{*}P < 0.05$ *vs.* the MALAT1-NC or miR-374a control group. SAP, severe acute pancreatitis; MALAT1, metastasis-associated lung adenocarcinoma transcript 1; miR, microRNA; RT-qPCR, reverse transcription-quantitative polymerase chain reaction; ANOVA, analysis of variance.

expression of genes both are targets of miR-374a and closely related to the inflammation in mice with low MALAT1 expression and found that only Sp1 showed the same trend as MALAT1 (**Figure 5B**). Similarly, we verified the targeting relationship between miR-374a and Sp1 by dual-luciferase experiments (**Figure 5C**). Sp1 expression was upregulated in the myocardial tissues of SAP mice (**Figure 5D**).

The MALAT1/miR-374a/Sp1 axis was involved in myocardial injury caused by SAP

To further validate the MALAT1/miR-374a/Sp1 axis in myocardial injury, mice were delivered with si-MALAT1 + miR-374a inhibitor and its control si-MALAT1 + miR-374a control, or miR-374a inhibitor + si-Sp1 and its control miR-374a inhibitor + Sp1-NC. The expression of miR-374a and Sp1 was detected in the myocardial tissues of mice to verify the efficiency of miR-374a inhibitor and si-Sp1 on genes (**Figure 6A**, **6B**). The inflammatory factor levels in myocardial tissues were increased by si-MALAT1 + miR-374a inhibitor relative to si-MALAT1 + miR-374a control and decreased by miR-374a inhibitor + si-Sp1 versus miR-374a inhibitor + Sp1-NC (**Figure 6C**). Downregulation of miR-374a deteriorated myocardial injury alleviated by si-MALAT1, and downregulation of Sp1 ameliorated myocardial injury exacerbated by miR-374a inhibitor (**Figure 6D**). HE staining was conducted to assess the structural changes in myocardial tissues, which presented that downregulation of miR-374a induced tissue edema and inflammatory infiltration, while lowering Sp1 had the opposite effect and alleviated myocardial tissue damage (**Figure 6E**). Inhibition of miR-374a decreased Bcl-2 and increased Bax expression in the presence of si-MALAT1, while downregulation of Sp1 repressed the effect of the miR-374a inhibitor (**Figure 6F**). Also, TUNEL-positive cells in tissues were increased by downregulation of miR-374a in

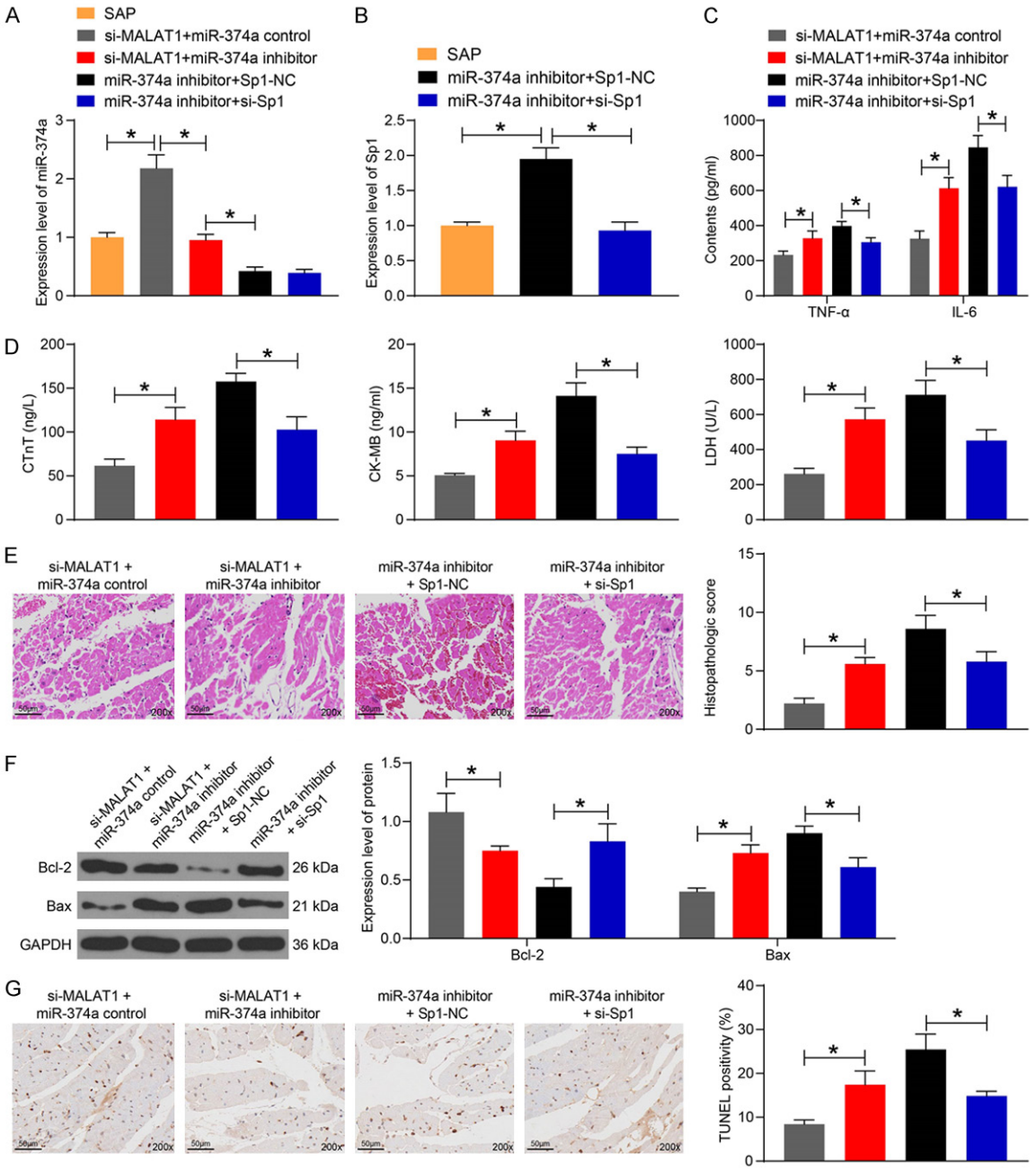

Figure 6. si-MALAT1 protected against myocardial injury in mice via the miR-374a/Sp1 axis. si-MALAT1 + miR-374a inhibitor or miR-374a inhibitor + si-Sp1 were delivered into SAP mice. (A) Quantification of miR-374a expression by RT-qPCR in SAP mice after delivery; (B) Quantification of Sp1 expression by RT-qPCR in SAP mice after delivery; (C) ELISA for the detection of inflammatory factors in the blood of mice; (D) ELISA for the detection of myocardial injury markers in myocardial tissue; (E) Observation of damage in myocardial tissue of SAP mice by HE staining; (F) Western blot detection of apoptotic proteins Bcl-2 and Bax in myocardial tissues of SAP mice; (G) Observation of cardiomyocyte apoptosis in myocardial tissues by TUNEL. n = 5. Measurement data were expressed as mean ± standard deviation; an unpaired *t-test* was performed for comparisons between two groups (B), and one-way (A, C, D and G) or two-way (F) ANOVA was performed for multiple-group comparison; the experiment was repeated three times. $^{*}P < 0.05$ *vs.* the SAP, si-MALAT1 + miR-374a control or miR-374a inhibitor + Sp1-NC group. SAP, severe acute pancreatitis; MALAT1, metastasis-associated lung adenocarcinoma transcript 1; miR, microRNA; RT-qPCR, reverse transcription-quantitative polymerase chain reaction; ELISA, enzyme-linked immunosorbent assays; ANOVA, analysis of variance.

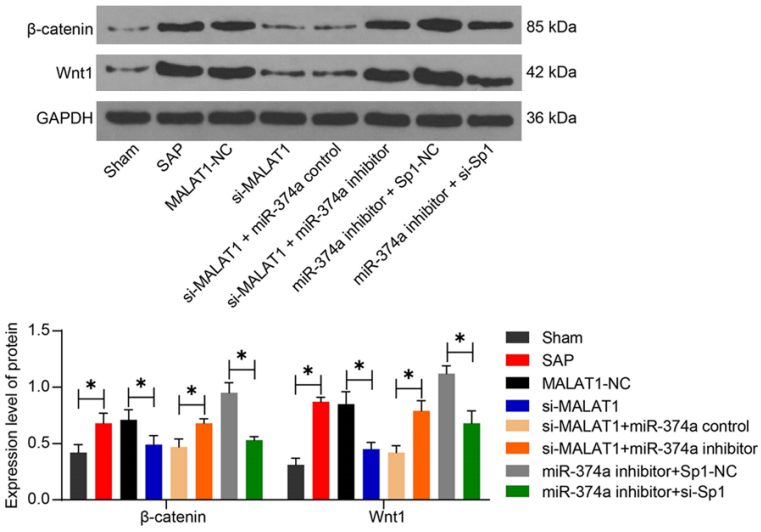

Figure 7. The Wnt/β-catenin signaling pathway was involved in the MALAT1/miR-374a/Sp1 axis-mediated myocardial injury in mice. Wnt1 and β-catenin protein expression in myocardial tissues of mice. n = 5. Measurement data were expressed as mean ± standard deviation; Two-way ANOVA was performed for multiple-group comparison; the experiment was repeated three times. $^{*}P < 0.05$ *vs.* the sham, MALAT1-NC, si-MALAT1 + miR-374a control or miR-374a inhibitor + Sp1-NC group. MALAT1, metastasis-associated lung adenocarcinoma transcript 1; miR, microRNA; ANOVA, analysis of variance.

the presence of si-MALAT1, whereas TUNEL-positive cells in tissues were increased by downregulation of Sp1 in the presence of miR-374a inhibitor (**Figure 6G**).

Sp1 contributed to myocardial injury by mediating the Wnt/β-catenin pathway

Finally, we investigated the pathway mediated by Sp1 and examined the expression of Wnt1 and β-catenin in myocardial tissues from mice with different treatments using Western blot (**Figure 7**). The Wnt/β-catenin pathway was activated in SAP mice relative to the sham-operated mice, while si-MALAT1 inhibited the Wnt/β-catenin pathway activity. Downregulation of miR-374a potentiated Wnt/β-catenin pathway activity in the presence of si-MALAT1, and downregulation of Sp1 reversed the action of miR-374a inhibitor to block the Wnt/β-catenin pathway. Overall, MALAT1/miR-374a/Sp1 axis affects myocardial injury by mediating the Wnt/β-catenin pathway.

Discussion

Acute pancreatitis (AP) is one of the most frequent causes of hospitalization for gastrointestinal diseases, with an annual incidence ranging from 5-30 cases per 100,000 population worldwide [14]. Treatment for mild AP patients only requires short hospitalization, while treatment for SAP patients often requires intensive care, making identifying SAP patients at an early stage a necessity for accomplishing optimal outcomes [15]. In term of multiple organ system dysfunctions of SAP, cardiovascular manifestations are the most frequent [16]. In this study, mice were injected with 5% sodium taurocholate to construct SAP mice *in vivo*. The expression of MALAT1 and Sp1 was overexpressed in the myocardial tissues of SAP mice, while miR-374a was downregulated. Besides, loss-of-function experiments were conducted to ascertain the functions of MALAT1, and rescue experiments were performed to construct a regulatory network among MALAT1, miR-374a, and Sp1. Our study expanded the insights to understand the pathogenesis of myocardial tissues in SAP.

MALAT1 has been reported to be significantly elevated in the myocardium of patients and rats with myocardial infarction, and MALAT1 knockdown suppressed apoptosis in rats with myocardial ischemia-reperfusion [17]. In the present study, overexpression of MALAT1 was identified in the myocardial tissues of SAP mice. In addition, downregulation of MALAT1 using siRNA significantly reduced apoptosis, inflammatory responses, and myocardial injuries in mice, as manifested by lowered TNF-α, IL-6, and Bax, and higher Bcl-2. Similarly, after MALAT1 knockdown in human vascular endothelial cells, it was found that the levels of TNF-α, IL-6, and Bax and apoptosis were decreased [18]. Consistent results were also observed in cells exposed to oxygen-glucose deprivation and reperfusion [19]. However, the downstream mechanism of MALAT1 in myocardial injuries is unclear and requires further investigation.

Recent evidence has uncovered that lncRNAs may act as ceRNAs, thus involved in organismal

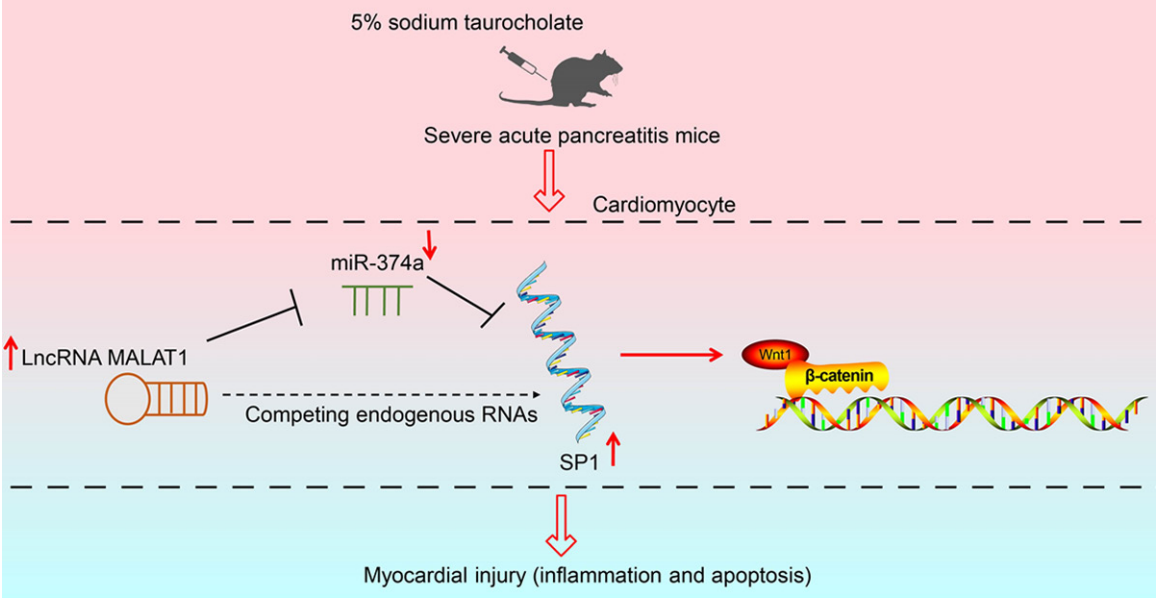

Figure 8. Schematic illustration of the role of MALAT1 in SAP-induced myocardial injury. LncRNA MALAT1 promotes the progression of SAP-related myocardial injury by blocking the inhibitory effect of miR-374a on Sp1 expression and activating the Wnt/β-catenin pathway. SAP, severe acute pancreatitis; lncRNA, long noncoding RNA, MALAT1, metastasis-associated lung adenocarcinoma transcript 1; miR, microRNA.

differentiation, and development in addition to cellular biology [20]. For example, the silencing of MALAT1 by siRNA attenuated heart damage in rats with acute myocardial infarction through the miR-125b-5p/NLCR5 axis [21]. As a consequence, we explored the downstream miRNA of MALAT1 in myocardial tissues of SAP mice using microarray analysis. miR-374a was found to be the most variable miRNA in myocardial tissues of SAP mice overexpressing MALAT1 or not, thereby being chosen as the target of our following studies. miR-374a-5p was identified to be reduced in a myocardial cell model and a mouse model of ischemia/reperfusion, and miR-374a-5p upregulation ameliorated myocardial cell damage *in vivo* and *in vitro* [22]. In the present study, miR-374a inhibitor was noted to reverse the repressive effects of si-MALAT1 on myocardial injuries.

Subsequently, five bioinformatics websites were utilized to predict the putative targets of miR-374a. An additional RT-qPCR was performed to reveal that only Sp1 was downregulated by si-MALAT1, indicating that MALAT1 may positively regulate Sp1 through binding to miR-374a. Sp1 is an 875-amino-acid, 100- to 110-kDa nuclear transcription factor that plays a regulatory role in apoptosis, inflammation, and other pathologic disorders [23]. More specifically, miR-374 has the potency to alleviate myocardial ischemia-reperfusion damage in a rat model by targeting Sp1 [24]. In addition, myocardial injuries, including elevated LDH release, were strongly aggravated by the overexpression of circular RNA Cdr1as, while the expression of Sp1 in heart tissues was upregulated consistently, which were all reversed by the restoration of miR-7a [25]. In our rescue experiments, the miR-374 inhibitor exacerbated cardiomyocyte apoptosis, inflammatory responses, and myocardial injuries, which were all antagonized by si-Sp1, substantiating the axis of MALAT1/miR-374/Sp1. Interestingly, MALAT1 knockdown ameliorated the myocardial injury in rats, which is probably correlated with the inhibitory effects of si-MALAT1 on β-catenin [26]. Therefore, we believed that the Wnt/β-catenin pathway was also involved in MALAT1/miR-374/Sp1-mediated myocardial injury. Our western blot assay corroborated that the Wnt/β-catenin pathway was activated in SAP mice, and positively regulated by miR-374 inhibitor, whereas negatively regulated by si-MALAT1 and si-Sp1. Still, more *in vitro* experiments are necessary to confirm the action of the MALAT1/miR-374/Sp1/Wnt/β-catenin axis.

Conclusion

This study demonstrated that MALAT1 was abnormally overexpressed in myocardial tissues after SAP. Silencing of MALAT1 inhibited cell apoptosis and inflammation to alleviate myocardial injuries, whereas miR-374a inhibitor reversed these effects. Moreover, MALAT1 sponged miR-374a and miR-374a bound to Sp1 to regulate the Wnt/β-catenin pathway. Taken together, we conclude that MALAT1 promotes myocardial injuries in SAP by activating the Sp1/Wnt/β-catenin pathway through sponging miR-374a (**Figure 8**), which provides a potential therapeutic target for ameliorating myocardial injuries in SAP.

Disclosure of conflict of interest

None.

Address correspondence to: Zhong Shen, Department of General Surgery, Jinshan Branch of Shanghai Sixth People's Hospital, Shanghai Jiaotong University, No. 147, Jiankang Road, Jinshan District, Shanghai 201599, P. R. China. Tel: +86-13801657944; Fax: +86-13801657944; E-mail: shenzhong1699@163.com

References

[1] Harper SJ and Cheslyn-Curtis S. Acute pancreatitis. Ann Clin Biochem 2011; 48: 23-37.
[2] Heckler M, Hackert T, Hu K, Halloran CM, Buchler MW and Neoptolemos JP. Severe acute pancreatitis: surgical indications and treatment. Langenbecks Arch Surg 2021; 406: 521-535.
[3] Zerem E. Treatment of severe acute pancreatitis and its complications. World J Gastroenterol 2014; 20: 13879-13892.
[4] Meyer A, Kubrusly MS, Salemi VM, De Mendonca Coelho AM, Molan NA, Patzina RA, Machado MC, Mady C, D'Albuquerque LA and Jukemura J. Severe acute pancreatitis: a possible role of intramyocardial cytokine production. JOP 2014; 15: 237-242.
[5] Schmitz SU, Grote P and Herrmann BG. Mechanisms of long noncoding RNA function in development and disease. Cell Mol Life Sci 2016; 73: 2491-2509.
[6] Zhao D, Ge H, Ma B, Xue D, Zhang W, Li Z and Sun H. The interaction between ANXA2 and lncRNA Fendrr promotes cell apoptosis in caerulein-induced acute pancreatitis. J Cell Biochem 2019; 120: 8160-8168.
[7] Li J, Bu X, Chen X, Xiong P, Chen Z and Yu L. Predictive value of long non-coding RNA intersectin 1-2 for occurrence and in-hospital mortality of severe acute pancreatitis. J Clin Lab Anal 2020; 34: e23170.
[8] Arun G, Diermeier S, Akerman M, Chang KC, Wilkinson JE, Hearn S, Kim Y, MacLeod AR, Krainer AR, Norton L, Brogi E, Egeblad M and Spector DL. Differentiation of mammary tumors and reduction in metastasis upon Malat1 lncRNA loss. Genes Dev 2016; 30: 34-51.
[9] Zhang M, Gu H, Xu W and Zhou X. Down-regulation of lncRNA MALAT1 reduces cardiomyocyte apoptosis and improves left ventricular function in diabetic rats. Int J Cardiol 2016; 203: 214-216.
[10] Gao Q and Wang Y. Long noncoding RNA MALAT1 regulates apoptosis in ischemic stroke by sponging miR-205-3p and modulating PTEN expression. Am J Transl Res 2020; 12: 2738-2748.
[11] Paraskevopoulou MD and Hatzigeorgiou AG. Analyzing miRNA-lncRNA interactions. Methods Mol Biol 2016; 1402: 271-286.
[12] Aho HJ, Nevalainen TJ, Lindberg RL and Aho AJ. Experimental pancreatitis in the rat. The role of phospholipase A in sodium taurocholate-induced acute haemorrhagic pancreatitis. Scand J Gastroenterol 1980; 15: 1027-1031.
[13] Rongione AJ, Kusske AM, Kwan K, Ashley SW, Reber HA and McFadden DW. Interleukin 10 reduces the severity of acute pancreatitis in rats. Gastroenterology 1997; 112: 960-967.
[14] Siregar GA and Siregar GP. Management of severe acute pancreatitis. Open Access Maced J Med Sci 2019; 7: 3319-3323.
[15] Liu P, Xia L, Zhang WL, Ke HJ, Su T, Deng LB, Chen YX and Lv NH. Identification of serum microRNAs as diagnostic and prognostic biomarkers for acute pancreatitis. Pancreatology 2014; 14: 159-166.
[16] Yegneswaran B, Kostis JB and Pitchumoni CS. Cardiovascular manifestations of acute pancreatitis. J Crit Care 2011; 26: 225, e11-8.
[17] Sun T, Cheng YT, Yan LX, Krittanawong C, Qian W and Zhang HJ. LncRNA MALAT1 knockdown alleviates myocardial apoptosis in rats with myocardial ischemia-reperfusion through activating PI3K/AKT signaling pathway. Eur Rev Med Pharmacol Sci 2019; 23: 10523-10531.
[18] Gong YP, Zhang YW, Su XQ and Gao HB. Inhibition of long noncoding RNA MALAT1 suppresses high glucose-induced apoptosis and inflammation in human umbilical vein endothelial cells by suppressing the NF-kappaB signaling pathway. Biochem Cell Biol 2020; 98: 669-675.
[19] Gong L, Chang H and Xu H. LncRNA MALAT1 knockdown alleviates oxygen-glucose depriva-

tion and reperfusion induced cardiomyocyte apoptotic death by regulating miR-122. Exp Mol Pathol 2019; 111: 104325.
[20] Hou J, Zhou C, Long H, Zheng S, Guo T, Wu Q, Wu H, Zhong T and Wang T. Long noncoding RNAs: novel molecules in cardiovascular biology, disease and regeneration. Exp Mol Pathol 2016; 100: 493-501.
[21] Liu Z, Liu J, Wei Y, Xu J, Wang Z, Wang P, Sun H, Song Z and Liu Q. LncRNA MALAT1 prevents the protective effects of miR-125b-5p against acute myocardial infarction through positive regulation of NLRC5. Exp Ther Med 2020; 19: 990-998.
[22] Huang ZQ, Xu W, Wu JL, Lu X and Chen XM. MicroRNA-374a protects against myocardial ischemia-reperfusion injury in mice by targeting the MAPK6 pathway. Life Sci 2019; 232: 116619.
[23] Li R, Geng HH, Xiao J, Qin XT, Wang F, Xing JH, Xia YF, Mao Y, Liang JW and Ji XP. miR-7a/b attenuates post-myocardial infarction remodeling and protects H9c2 cardiomyoblast against hypoxia-induced apoptosis involving Sp1 and PARP-1. Sci Rep 2016; 6: 29082.
[24] Zhang SB, Liu TJ, Pu GH, Li BY, Gao XZ and Han XL. MicroRNA-374 exerts protective effects by inhibiting SP1 through activating the PI3K/Akt pathway in rat models of myocardial ischemia-reperfusion after sevoflurane preconditioning. Cell Physiol Biochem 2018; 46: 1455-1470.
[25] Geng HH, Li R, Su YM, Xiao J, Pan M, Cai XX and Ji XP. The circular RNA Cdr1as promotes myocardial infarction by mediating the regulation of miR-7a on its target genes expression. PLoS One 2016; 11: e0151753.
[26] Xu XZ, Luo B, Xiao Y and Zheng WQ. Effects of lncRNA MALAT1-mediated beta-catenin signaling pathway on myocardial cell apoptosis in rats with myocardial ischemia/reperfusion injury. Eur Rev Med Pharmacol Sci 2019; 23: 9557-9565.